Publishing Excellence Inspiring Progress
ARISTON PUBLICATIONS
MatSci Express
ISSN: 2997-8440 www.aristonpubs.com/matsci-express https://doi.org/10.69626/mse.2025.0218

RESEARCH ARTICLE

A Highly Sensitive ZnCOx/Nickel Foam Nanocomposite Electrode for Electrochemical Magnesium Ion Detection

S. K. Pawar, N. A. Wadodkar, A. S. Pathak, R. S. Salunke, D. J. Shirale*

ABSTRACT: This study presents the development and application of a novel electrochemical sensor for the detection of magnesium ions (Mg^{2+}), a critical nutrient in agricultural and environmental systems. The sensor was fabricated by synthesizing a zinc cobalt oxide (ZnCOx) nanocomposite directly onto a three-dimensional nickel foam substrate via a controlled hydrothermal method. The choice of nickel foam as a scaffold was strategic, leveraging its high porosity, extensive surface area, and excellent electrical conductivity to facilitate efficient electron transfer and provide a robust platform for nanocomposite growth. The resulting ZnCOx material exhibited a unique nanowire bundle-like morphology, as confirmed by field emission scanning electron microscopy (FESEM), which significantly increases the density of available electroactive sites. The electrochemical performance of the modified electrode was rigorously characterized using cyclic voltammetry and electrochemical impedance spectroscopy, which revealed favorable redox activity and low charge transfer resistance. For the detection of Mg^{2+}, square wave voltammetry was employed under optimized conditions of pH, potential, and electrolyte composition. The sensor demonstrated a linear response to magnesium ion concentration with a high sensitivity of 3.44 µA/µM and a low detection limit of 7.25 µM. The exceptional performance is attributed to the synergistic combination of the catalytic ZnCOx nanocomposite and the conductive nickel foam matrix. This work establishes the ZnCOx/Ni-foam electrode as a promising, reliable, and efficient tool for the precise monitoring of magnesium levels, with direct implications for advancing precision agriculture and environmental diagnostics.

Keywords: Magnesium ion detection, Electrochemical sensor, Zinc cobalt oxide, Nanocomposite, Square wave voltammetry, Nickel foam

Received: 02 February 2025; Revised: 07 May 2025; Accepted: 05 June 2025; Published Online: 02 July 2025

1. INTRODUCTION

Magnesium (Mg) is an essential macronutrient for plant growth and development, playing a critical role in photosynthesis as a central component of the chlorophyll molecule. In addition to its photosynthetic function, magnesium is involved in protein synthesis, enzyme activation, and the structural stability of ribosomes. The productivity and overall health of plants are significantly influenced by magnesium availability in soil [1]. The concentration of magnesium is governed by several soil-related parameters, including the parent material, texture, pH, cation exchange capacity (CEC), and organic matter content. Soils derived from magnesium-rich parent rocks, such as dolomite or basalt, tend to exhibit higher native magnesium content. Conversely, sandy soils, due to their low CEC and high leaching potential, often exhibit reduced magnesium levels compared to clay-rich soils. Magnesium availability decreases markedly in acidic soils (pH < 5.5), primarily due to enhanced solubility and leaching losses. Liming such soils can help improve magnesium retention. Soils with higher CEC can retain more magnesium ions, thereby minimizing leaching. The addition of organic matter contributes to better

Nanostructured Materials Processing Laboratory, Department of Electronics, Kavayitri Bahinabai Chaudhari North Maharashtra University, Jalgaon – 425001, Maharashtra, India.

* Author to whom correspondence should be addressed: shiraledj@gmail.com (D. J. Shirale)

© Ariston Publications 2025. All rights reserved.

soil structure and water retention, indirectly enhancing magnesium availability [2, 3]. Magnesium deficiency is characterized by symptoms such as interveinal chlorosis in older leaves, stunted growth, and reduced crop yield. These symptoms are commonly observed in sandy, acidic soils with elevated concentrations of competing cations like calcium and potassium. Although rare, excessive levels of magnesium may also pose agronomic issues by interfering with the uptake of other essential cations.

Routine soil testing is essential for monitoring magnesium concentrations and guiding fertilizer application strategies. Amendments such as dolomitic lime (magnesium carbonate) can simultaneously correct soil acidity and supply magnesium. Other common fertilizers include magnesium sulfate (Epsom salt), magnesium oxide, and magnesium chloride, which are applied based on soil analysis data. Organic matter amendments can further improve magnesium availability by enhancing nutrient retention and microbial activity [4, 5]**.** A range of analytical techniques has been developed to quantify magnesium in soils. Classical methods such as chromatography, high-performance liquid chromatography (HPLC) [6], and optical spectroscopy [7] offer accurate measurements but are often limited by their complexity, cost, and the need for sophisticated instrumentation and skilled personnel. Consequently, there is a growing interest in developing rapid, cost-effective sensing technologies for real-time soil nutrient assessment. Among these, electrochemical sensors have gained considerable attention due to their portability, high sensitivity, and operational simplicity. Electrochemical sensors function based on ionic interactions at the sensing surface, and their performance is highly dependent on the materials used in their fabrication. The type of sensing material influences critical parameters such as detection limit, response time, and selectivity [8-12]. Traditional approaches such as Atomic Absorption Spectroscopy (AAS) and Inductively Coupled Plasma Optical Emission Spectroscopy (ICP-OES) remain widely used for soil magnesium analysis. AAS operates by digesting soil samples in acidic solutions and measuring the absorbance of magnesium atoms, while ICP-OES quantifies magnesium based on emission intensity at characteristic wavelengths following plasma excitation. Flame photometry, though largely outdated, operates on a similar principle, assessing emission at the magnesium-specific wavelength [13-16]. X-ray fluorescence (XRF) spectroscopy allows direct, non-destructive elemental analysis by measuring secondary X-rays emitted by soil components when exposed to primary radiation. Colorimetric methods, involving the formation of colored complexes with magnesium-specific reagents, provide an accessible alternative, with quantification via spectrophotometry. Ion-selective electrodes (ISEs) with magnesium-sensitive membranes offer yet another route for real-time ionic activity measurements [17-19].

Despite the variety of available methods, there is an ongoing demand for miniaturized, field-deployable sensors with enhanced sensitivity and selectivity for magnesium detection [20-22]. In this context, nanomaterials have emerged as promising candidates for sensor development. Their high surface-area-to-volume ratio, tunable surface chemistry, and strong electrochemical activity make them suitable for detecting trace amounts of Mg^{2+} in complex soil matrices. Nanostructured materials, such as carbon dots, graphene derivatives, carbon nanotubes, and metal oxides, are capable of interacting selectively with magnesium ions, often through surface adsorption, complexation, or ion exchange mechanisms. These interactions can be transduced into measurable electrical or optical signals via various mechanisms, including chemiresistive, fluorescent, and electrochemical detection [23, 24]. Optical sensors based on nanomaterials detect magnesium through changes in fluorescence or absorbance, often triggered by ligand-functionalized nanoparticles interacting with Mg^{2+} ions. For instance, carbon-based fluorescent sensors can emit light at specific wavelengths upon magnesium binding. Electrochemical sensors, on the other hand, detect changes in current or potential arising from the redox activity of magnesium ions at the sensor interface. Nanocomposites that integrate multiple materials often outperform single-component systems by enhancing conductivity, signal stability, and target specificity [25]. Among the many nanomaterials explored, zinc cobalt oxide ($ZnCo_2O_4$) has shown particular promise due to its advantageous structural, electrical, and catalytic properties. $ZnCo_2O_4$ adopts a spinel-type structure, conferring a high surface area and excellent redox characteristics, while the synergistic effect of Zn and Co oxides enhances overall conductivity and electrochemical performance. These features make $ZnCo_2O_4$ an attractive candidate for magnesium ion sensing [26, 27].

In the present work, we report the fabrication of a $ZnCo_2O_4$ (denoted as ZnCOx) nanocomposite-based electrochemical sensor for the detection of magnesium in soil. The ZnCOx material was synthesized via a hydrothermal method and deposited onto a porous nickel foam substrate, which serves as a conductive scaffold with high surface area. Process parameters including applied potential, deposition time, electrolyte composition, and pH were optimized to enhance sensor response. The resulting sensor exhibited high selectivity and sensitivity toward Mg^{2+} ions, with performance metrics suitable for practical soil monitoring applications. This study underscores the potential of ZnCOx-based nanocomposites as effective sensing platforms for real-time soil nutrient analysis, contributing to precision agriculture and sustainable soil management practices.

2. EXPERIMENTAL DETAILS

2.1. Materials and characterization methods

All reagents used in this study were of analytical grade and employed without further purification. Zinc nitrate hexahydrate ($Zn(NO_3)_2{\cdot}6H_2O$), cobalt nitrate hexahydrate ($Co(NO_3)_2{\cdot}6H_2O$), ammonium persulfate ($(NH_4)_2S_2O_8$), sodium hydroxide (NaOH), potassium hydroxide (KOH), hydrochloric acid (HCl), potassium dihydrogen phosphate

© Ariston Publications 2025. All rights reserved.

(KH_2PO_4), and urea were procured from standard commercial sources. Nickel foam sheets (dimensions: 200 mm × 300 mm) were purchased from Vritra Technologies, New Delhi, India. Experimental procedures were carried out using freshly prepared ultra-pure water throughout.

Equipment employed for the synthesis and treatment of materials included an ultrasonicator, a muffle furnace (Zexter Lab Solutions, India), and a vacuum oven (Raj Scientific Industries, Mumbai, India). The crystalline phase of the synthesized ZnCOx nanocomposite was characterized using X-ray diffraction (XRD) with Cu-Kα radiation (λ = 1.5406 Å) over a 2θ range of 20° to 90°. Morphological features and elemental composition were examined using field emission scanning electron microscopy (FESEM) coupled with energy-dispersive X-ray spectroscopy (EDS). Electrochemical measurements, including cyclic voltammetry (CV), square wave voltammetry (SWV), and electrochemical impedance spectroscopy (EIS), were performed using a Biologic SP-150 electrochemical workstation (BioLogic Science Instruments, France).

2.2. Synthesis of ZnCOx nanocomposite

The ZnCOx nanocomposite was synthesized via a hydrothermal approach, employing a controlled reaction between metal precursors and a structure-directing agent in aqueous solution. In a typical synthesis, 6 mM cobalt nitrate hexahydrate ($Co(NO_3)_2 \cdot 6H_2O$), 3 mM zinc nitrate hexahydrate ($Zn(NO_3)_2 \cdot 6H_2O$), 12 mM urea ($CO(NH_2)_2$), and 4 mM ammonium persulfate ($(NH_4)_2S_2O_8$) were dissolved in 80 mL of deionized water under continuous stirring. Urea served as a controlled source of hydroxide ions upon thermal decomposition, facilitating uniform co-precipitation of metal hydroxides. Ammonium persulfate acted as a mild oxidant to assist in the formation of the mixed metal oxide phase. A pre-cleaned piece of nickel foam (serving as both substrate and current collector) was immersed in the homogeneous solution. The mixture was then transferred into a 100 mL Teflon-lined stainless-steel autoclave, sealed, and heated at 130 °C for 5 hours in a muffle furnace. The hydrothermal conditions promoted in situ nucleation and growth of the ZnCOx precursor directly onto the surface of the nickel foam, resulting in uniform deposition with good interfacial contact. Upon completion of the reaction, the coated nickel foam was removed from the autoclave, rinsed thoroughly with deionized water to eliminate unreacted species, followed by ethanol to remove organic residues. The samples were subsequently dried in a vacuum oven at 60 °C for 5 hours to eliminate residual moisture. The final step involved calcination at 300 °C for 1 hour in air, which transformed the intermediate hydroxide phases into a stable, crystalline ZnCOx nanocomposite. This thermal treatment improved the structural integrity and electrochemical performance of the material. The resulting ZnCOx-coated nickel foam was retained for subsequent structural characterization and electrochemical sensing experiments, as illustrated in Figure 1.

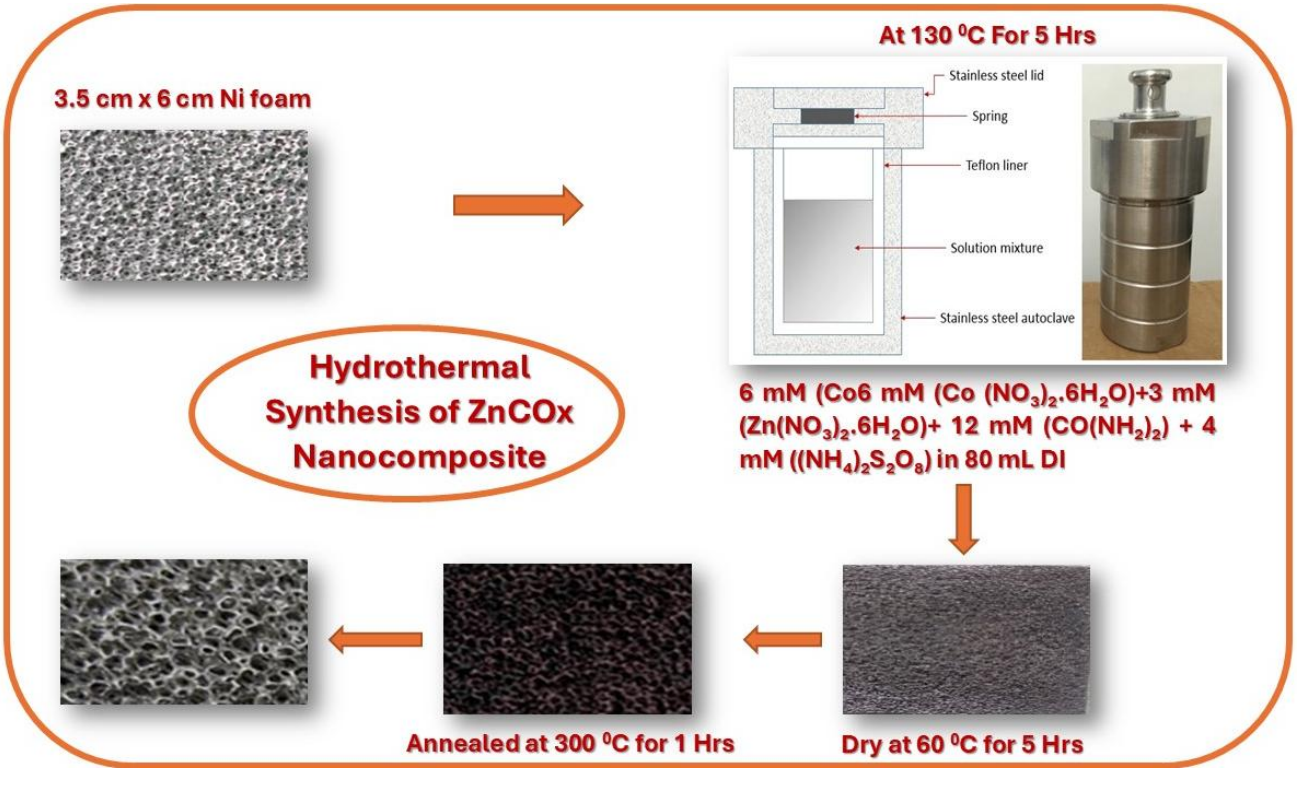

Fig. 1. Schematic illustration of the hydrothermal synthesis process for $ZnCO_x$ nanocomposite.

© Ariston Publications 2025. All rights reserved.

2.3. Electrochemical measurements

The electrochemical performance of the synthesized ZnCOx-modified electrode was evaluated using cyclic voltammetry (CV) and electrochemical impedance spectroscopy (EIS). All measurements were conducted in a conventional three-electrode configuration comprising ZnCOx-coated nickel foam as the working electrode, a platinum wire as the counter electrode, and an Ag/AgCl (3 M KCl) electrode as the reference. The experiments were carried out in 1 M KOH aqueous electrolyte. Cyclic voltammetry was performed over a potential range of 0.0 V to 0.6 V (vs. Ag/AgCl) at a scan rate of 50 mV s^{-1} for 50 consecutive cycles. The CV profiles, shown in Figure 2(a), exhibit distinct anodic and cathodic peaks, indicative of well-defined and reversible redox processes occurring at the ZnCOx surface. The nearly symmetric shape of the curves and the minimal peak separation suggest favourable redox kinetics and electrochemical reversibility, characteristics beneficial for applications such as energy storage and sensing.

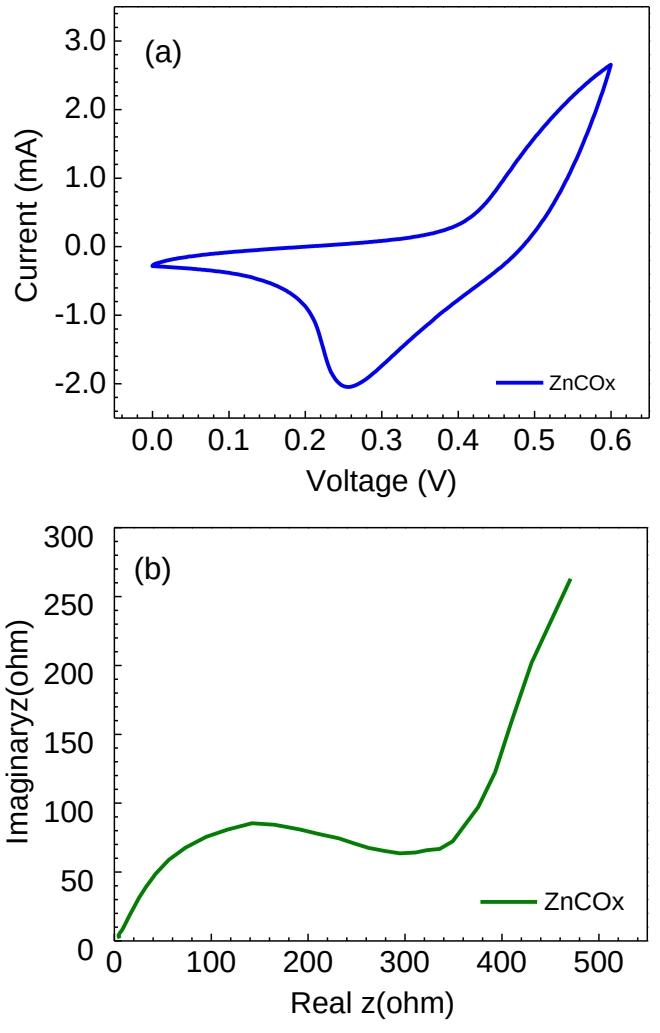

Fig. 2. (a) Cyclic voltammetry (CV) and (b) electrochemical impedance spectroscopy (EIS) characterization of $ZnCO_x$-modified nickel foam electrode in 1 M KOH solution.

Electrochemical impedance spectroscopy was conducted over a frequency range of 100 kHz to 100 Hz using a sinusoidal amplitude of 5 mV. The Nyquist plot (Figure 2(b)) reveals a semicircular region in the high-frequency domain followed by a linear portion in the low-frequency region. The high-frequency semicircle corresponds to the charge transfer resistance (R_{ct}) and double-layer capacitance (C_{dl}) at the electrode–electrolyte interface, while the inclined linear tail at lower frequencies reflects diffusion-related processes, often associated with ion transport limitations within the porous ZnCOx layer or the electrolyte. These electrochemical characteristics affirm that the ZnCOx-modified electrode exhibits favourable charge transfer properties and capacitive behaviour, making it a promising candidate for sensor-based applications.

3. RESULT AND DISCUSSION

3.1. FESEM and EDS analysis

The surface morphology of the cobalt oxide-modified nickel foam was examined using field emission scanning electron microscopy (FESEM). As shown in Figure 3(a), the micrograph reveals a disordered, coiled network of nanowire-like structures distributed across the surface of the nickel foam substrate. The formation of these nanowires is attributed to the hydrothermal reaction involving cobalt nitrate, urea, and ammonium persulfate in an alkaline aqueous medium. During synthesis, the gradual decomposition of urea releases hydroxide ions, leading to the initial formation of cobalt hydroxide nanosheets. These nanosheets subsequently transform into one-dimensional nanowires upon hydrothermal treatment. Ammonium persulfate serves as a mild oxidizing agent, facilitating the conversion of hydroxides into cobalt oxide. The irregular bundling and entanglement of the nanowires may be influenced by various synthesis parameters, including the concentration of precursors, pH of the reaction medium, temperature, and reaction duration [28].

Similar disordered nanowire architectures have been reported in previous studies and are of interest for their potential in catalysis, sensing, and energy storage applications. To enhance nanowire alignment and morphological uniformity, several strategies have been explored, such as the incorporation of surfactants, optimization of hydrothermal conditions, and post-synthetic thermal or chemical treatments. For instance, the use of cetyltrimethylammonium bromide (CTAB) as a structure-directing agent has been demonstrated to yield well-aligned cobalt oxide nanowires with improved uniformity and surface coverage on nickel foam substrates [29, 30]. Elemental analysis of the synthesized material was performed using energy-dispersive X-ray spectroscopy (EDS). The EDS spectrum (Figure 3(b)) confirms the presence of cobalt (Co), oxygen (O), and nickel (Ni), consistent with the formation of a cobalt oxide coating on the nickel foam framework.

© Ariston Publications 2025. All rights reserved.

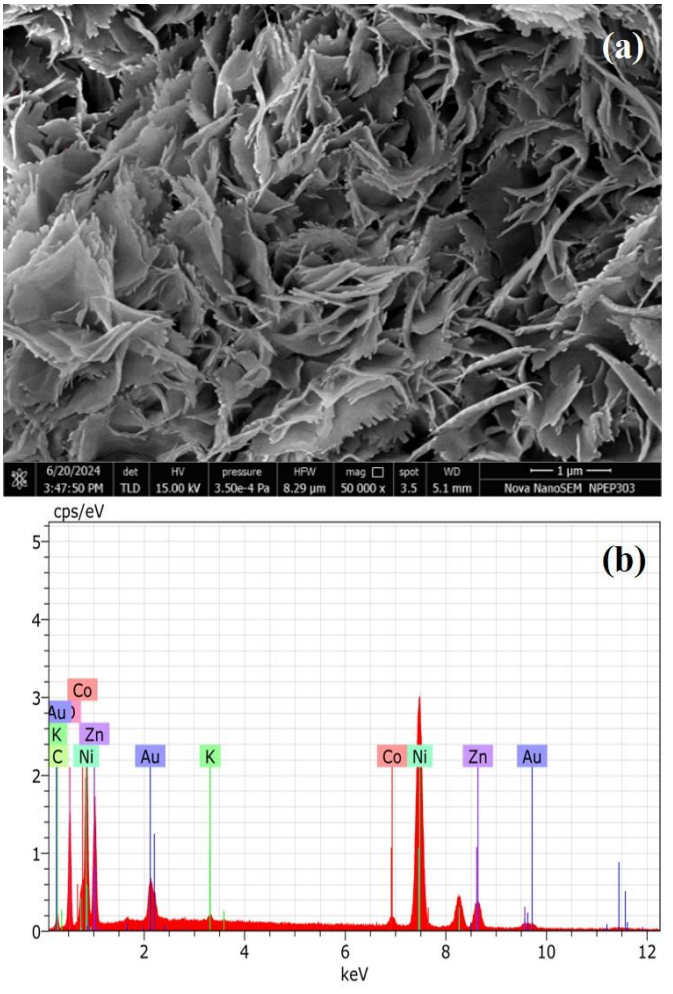

Fig. 3. (a) Field emission scanning electron microscopy (FESEM) image and (b) energy-dispersive X-ray spectroscopy (EDS) spectrum of the $ZnCO_x$ nanocomposite.

3.2. XRD analysis of ZnCOx nanocomposite

X-ray diffraction (XRD) was employed to investigate the crystallographic structure of the ZnCOx nanocomposite deposited on the nickel foam substrate. The resulting diffraction pattern, shown in Figure 4, indicates the successful formation of a mixed-phase metal oxide system with well-defined crystalline features. Prominent diffraction peaks corresponding to zinc oxide (ZnOx) were observed, with a notable reflection at a 2θ value of approximately 36.4°, assigned to the (101) plane of hexagonal ZnOx. This matches the standard pattern reported in the JCPDS database (Card No. 36-1451), confirming the presence of the wurtzite phase of ZnOx within the composite.

In addition to the ZnOx peaks, the XRD pattern exhibited several reflections attributable to cobalt oxide (CoOx) phases. Notably, diffraction peaks indexed to the (211), (511), and (220) planes were observed, consistent with the spinel-type structure of cobalt oxide (Co_3O_4), as referenced in JCPDS Card No. 42-1467. The detection of these reflections indicates the incorporation of crystalline CoOx phases into the material, further supporting the formation of a bimetallic oxide composite.

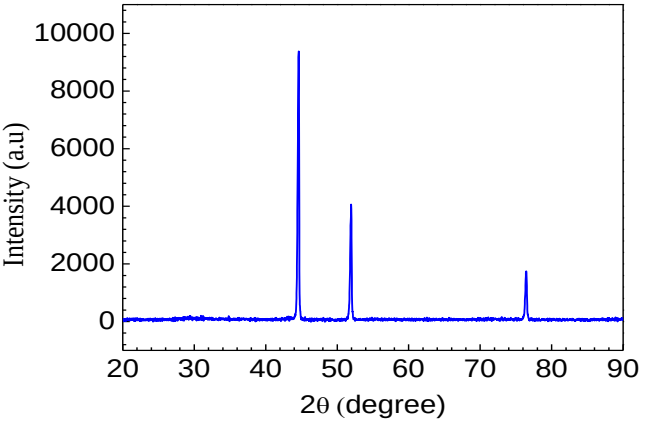

Fig. 4. X-ray diffraction (XRD) pattern of the ZnCOx nanocomposite deposited on nickel foam.

The coexistence of ZnOx and CoOx phases within the nanocomposite confirms the successful synthesis of a heterostructure material, herein referred to as ZnCOx. The presence of sharp and distinct diffraction peaks throughout the pattern suggests high crystallinity and phase purity of the deposited material. The integration of both hexagonal ZnOx and spinel CoOx within the composite is expected to facilitate improved electrochemical performance, owing to the complementary electronic and structural properties of the two oxide phases. These results confirm the formation of a well-crystallized ZnCOx nanocomposite coating on the nickel foam substrate, suitable for further application in electrochemical sensing systems.

3.3. Optimizing the experimental parameters

The performance of electrochemical sensors is highly dependent on the optimization of operational parameters, especially in applications requiring precise detection and quantification. For the ZnCOx nanocomposite-based electrode, key factors such as the pH of the electrolyte, applied potential, accumulation time, and ionic strength were systematically studied to determine their influence on the sensor's response toward magnesium ion detection. Each of these parameters has a direct impact on the interfacial processes occurring at the electrode surface, including analyte adsorption, redox kinetics, and overall signal intensity. Deviations from suitable conditions can lead to diminished current response, reduced sensitivity, or interference from competing species. As such, establishing appropriate experimental conditions is essential for achieving consistent and reproducible analytical results.

Square wave voltammetry (SWV) was selected as the method for parameter optimization due to its high sensitivity and rapid acquisition capability. By varying the experimental

© Ariston Publications 2025. All rights reserved.

conditions, current responses were recorded and analyzed to identify the optimal pH range, potential window, deposition time, and supporting electrolyte concentration. The conditions that produced the highest and most stable peak currents were selected for further measurements. This systematic optimization led to a marked enhancement in the electrochemical response of the sensor, thereby improving its applicability for reliable magnesium ion detection in complex matrices such as soil samples [31, 32].

3.3.1. Effect of supporting Electrolytes

The supporting electrolyte plays a crucial role in ensuring effective ionic conductivity within the electrochemical cell, facilitating the flow of current between the working and reference electrodes. In the absence of a supporting electrolyte, the solution exhibits high resistance, which can severely compromise current flow and result in distorted or unreliable electrochemical signals [33]. Beyond conductivity, supporting electrolytes serve to minimize analyte ion migration under the influence of an electric field. By maintaining a high concentration of inert ions in the solution, the supporting electrolyte ensures that mass transport of the analyte occurs primarily via diffusion. This leads to improved control over the electrochemical response and sharper, more well-defined peaks in Voltammetric measurements [34].

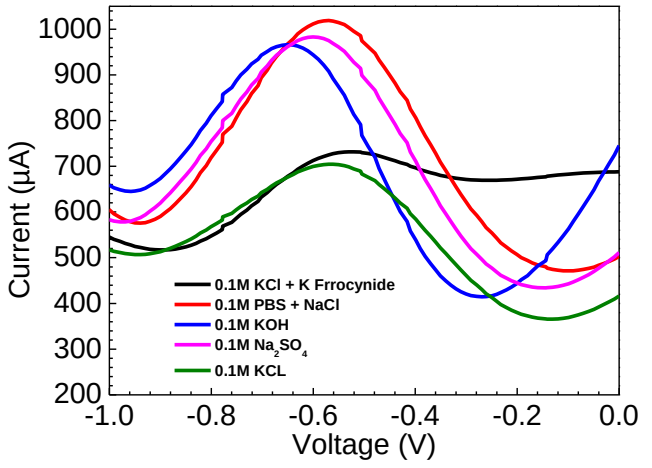

Fig. 5. Square wave voltammetry (SWV) response for different supporting electrolytes to evaluate the optimal medium for magnesium ion detection.

Additionally, supporting electrolytes often contribute to maintaining a stable pH, which is vital for reproducibility and accuracy. Fluctuations in pH can alter the redox properties of the analyte or influence the surface chemistry of the electrode, potentially affecting sensor performance and signal stability [34]. In the present study, various electrolytes were evaluated to assess their influence on the electrochemical response of magnesium ions. These included 0.1 M phosphate-buffered saline (PBS) adjusted with NaCl, 0.1 M potassium chloride (KCl), 0.1 M potassium ferrocyanide in KCl ($K_4[Fe(CN)_6]\cdot 3H_2O$ + KCl), 0.1 M sodium sulfate (Na_2SO_4), and 0.1 M potassium hydroxide (KOH). Among the tested systems, the PBS + NaCl electrolyte exhibited the most pronounced and well-defined magnesium reduction peak. As shown in Figure 5, this electrolyte system provided superior peak sharpness and intensity, indicating its suitability for the sensitive and selective detection of magnesium ions.

3.3.2. Influence of Potential Range and Immersion Time

In electrochemical sensing, careful selection of the potential window and adsorption time is crucial to achieve high signal intensity and reliable detection. The applied potential determines the driving force for electrochemical reactions and influences the kinetics of ion transfer at the electrode interface. If the potential is too low, electron transfer may be insufficient to initiate the redox reaction. On the other hand, excessively negative potentials can result in unwanted side reactions, such as hydrogen evolution, which compromise the selectivity and stability of the measurement system. To determine the most suitable deposition potential for magnesium ion detection using the ZnCOx-modified nickel foam electrode, the potential was varied between −0.9 V and −2.0 V while keeping the adsorption time constant. The peak current gradually increased with increasing negative potential and reached a maximum at −1.7 V, as shown in Figure 6(a). This potential provided a sufficient driving force for the electrochemical accumulation of Mg^{2+} ions on the electrode surface without inducing parasitic reactions. Beyond −1.7 V, a decline in current response was observed, likely due to competing processes such as water reduction or electrode surface instability. Thus, −1.7 V was selected as the optimal deposition potential. Following this, the adsorption time was optimized by varying it from 10 to 60 seconds at the fixed potential of −1.7 V.

As depicted in Figure 6(b), the peak current increased with longer adsorption times, indicating enhanced accumulation of Mg^{2+} ions on the electrode surface. The current reached its highest value at 40 seconds, suggesting that sufficient ion loading was achieved within this period. Extending the adsorption time beyond 40 seconds did not lead to further improvement and resulted in overlapping or plateauing of current signals, attributed to surface saturation or diffusion limitations. Therefore, an adsorption time of 40 seconds was identified as the most effective for achieving maximum sensitivity without compromising measurement reproducibility. These optimized parameters—an applied potential of −1.7 V and adsorption time of 40 seconds—were found to provide the most favourable conditions for the preconcentration of magnesium ions, enhancing the electrochemical response of the ZnCOx-modified electrode and ensuring consistent analytical performance.

3.3.3. Influence of pH

The pH of the supporting electrolyte plays a critical role in

© Ariston Publications 2025. All rights reserved.

electrochemical sensing by influencing both the physicochemical state of the analyte and the surface properties of the electrode. Variations in pH can alter the ionization state of the analyte and impact the stability, composition, and charge distribution of surface oxides on metal-based electrodes. Such changes directly affect electron transfer kinetics and, consequently, the sensitivity and selectivity of the sensor system [34-36]. To evaluate the influence of pH on the electrochemical behavior of magnesium ions at the ZnCOx-modified nickel foam electrode, experiments were conducted over a pH range of 6.0 to 7.5 using phosphate buffer as the supporting electrolyte.

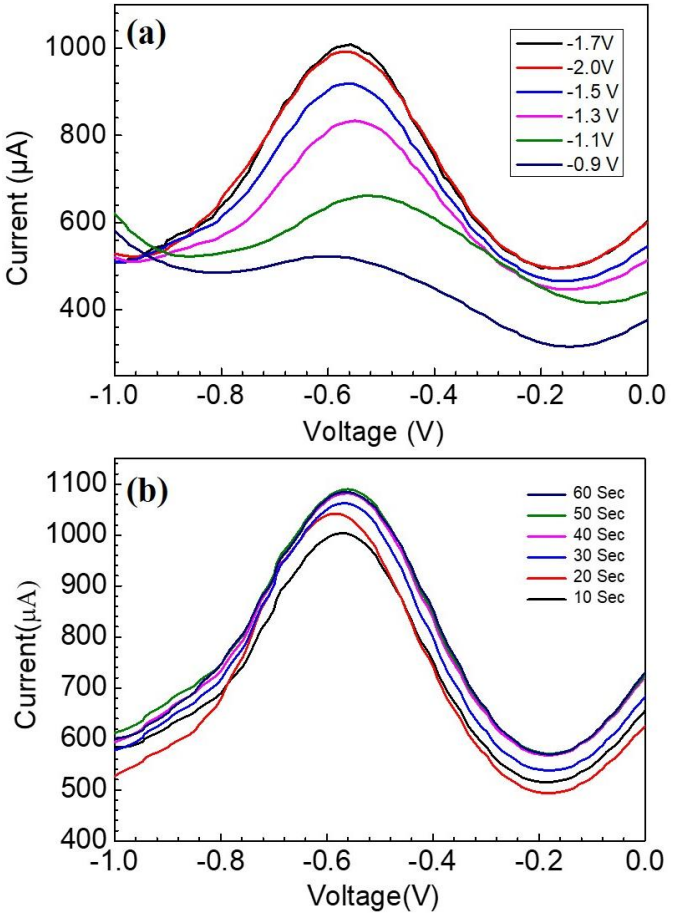

Fig. 6. Square wave voltammetry (SWV) response for (a) applied potential optimization and (b) accumulation time variation at fixed potential.

As shown in Figure 7, the oxidation peak current progressively increased with rising pH, reaching a maximum at pH 7.2. This enhancement suggests improved interaction between Mg^{2+} ions and the electrode surface under near-neutral conditions. The increase in current is likely due to more favorable electrode surface chemistry at this pH, which supports better adsorption and electron transfer. Beyond pH 7.2, a plateau or slight decline in current was observed, possibly due to changes in the hydration shell of magnesium ions or minor shifts in surface speciation that reduce the efficiency of charge transfer. Therefore, pH 7.2 was identified as the optimal condition, offering the most favorable environment for magnesium ion detection while maintaining the stability of the electrode and the electrolyte system. This pH value was used in subsequent experiments to ensure consistent and reproducible electrochemical performance.

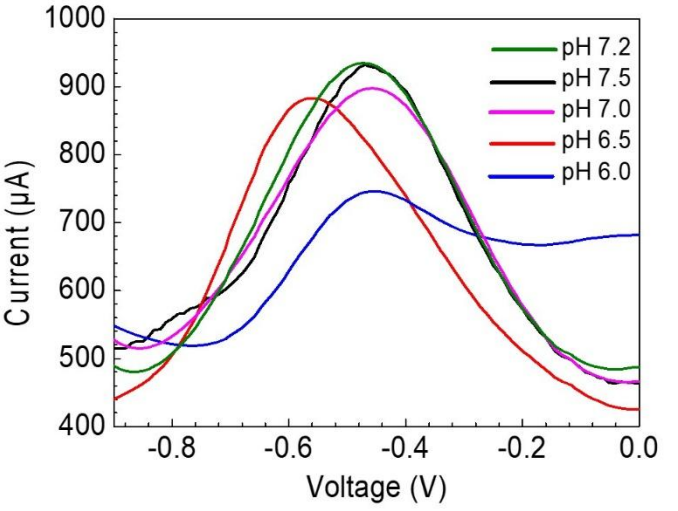

Fig. 7. Square wave voltammetry (SWV) response of the ZnCOx electrode at different pH levels to determine the optimal pH for magnesium sensing.

3.4. Electrochemical detection of Magnesium by using prepared ZnCOx nanocomposite decorated Ni-foam electrode

The adsorption of Mg^{2+} ions onto the $ZnCo_x$-modified nickel foam electrode significantly affects the electrode's surface charge distribution and electrochemical behavior. When Mg^{2+} ions interact with the composite surface, particularly through partial substitution of Zn^{2+} in the $ZnCO_3$ matrix, alterations in local electronic structure and conductivity may occur. These changes can be effectively monitored through electrochemical methods such as square wave voltammetry (SWV), which is sensitive to variations in charge transfer resistance and current response associated with surface interactions [37- 40].

In the present study, SWV was employed to assess the electrochemical response of the $ZnCo_x$/Ni-foam electrode toward various concentrations of Mg^{2+} ions prepared in a mixed electrolyte of 0.1 M phosphate buffer saline (PBS) and 0.2 M NaCl. As depicted in Figure 8, the most prominent oxidation peak was recorded at a potential of –0.56 V. This peak position is indicative of a favourable electrochemical reaction pathway at this potential, likely related to magnesium's oxidation on the modified electrode surface.

A clear and well-defined linear relationship was observed between the oxidation peak current and the increasing concentration of magnesium ions, as illustrated in Figure 9. The current response increased proportionally with

© Ariston Publications 2025. All rights reserved.

magnesium concentration, suggesting uniform surface adsorption and consistent charge transfer processes across the studied range. This linear behaviour confirms the electrode's reliability and reproducibility in detecting Mg^{2+} levels in solution.

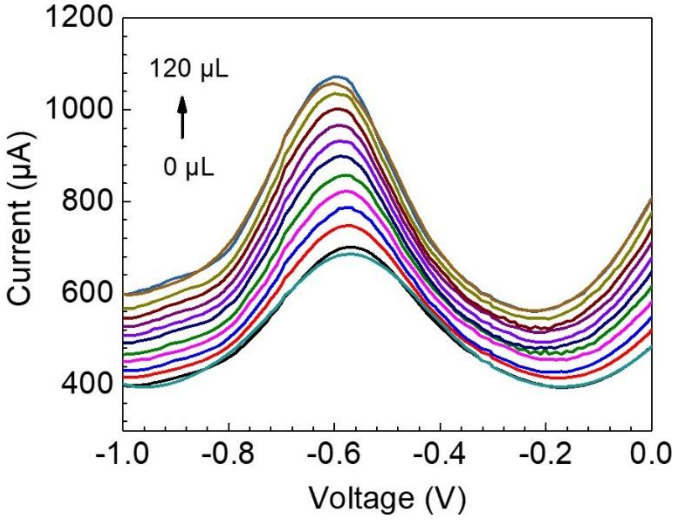

Fig. 8. Square wave voltammetry (SWV) response of $ZnCO_x$-modified nickel foam electrode with increasing concentrations of magnesium ions (Mg^{2+}).

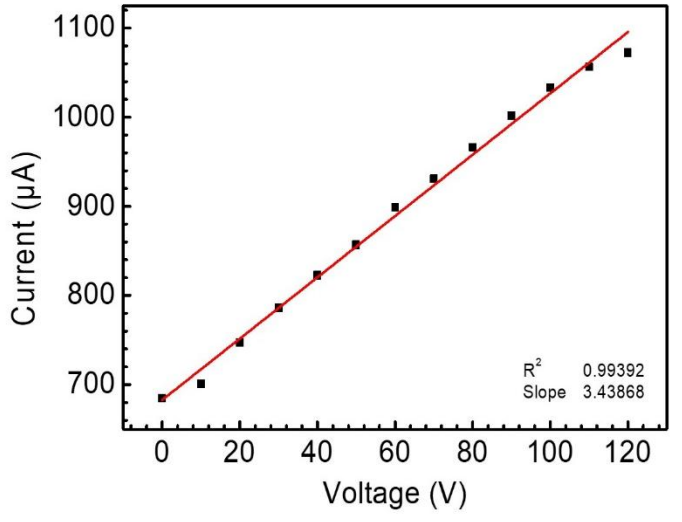

Fig. 9. Calibration curve depicting the electrochemical response of the $ZnCo_x$ nanocomposite-modified nickel foam electrode for the detection of magnesium ions (Mg^{2+}).

The calculated sensitivity of the sensor was 3.44 µA/µM, reflecting a high level of responsiveness to changes in analyte concentration. This value indicates that even small variations in magnesium content lead to measurable changes in current, underscoring the potential of the ZnCOx/Ni-foam electrode for trace-level detection. Furthermore, the limit of detection (LOD) was determined to be 7.25 µM, based on the signal-to-noise ratio (S/N = 3) derived from the calibration curve. This low LOD highlights the electrode's capacity to detect magnesium ions at biologically and environmentally relevant concentrations, making it a promising platform for real-sample applications such as soil and water analysis.

4. CONCLUSION

In summary, this study reports the successful fabrication and characterization of a novel electrochemical sensor based on ZnCOx nanowire bundles grown on a nickel foam substrate for the selective detection of magnesium ions (Mg^{2+}). The morphological and compositional features of the synthesized ZnCOx nanocomposite were thoroughly examined using field emission scanning electron microscopy (FESEM) and energy-dispersive X-ray spectroscopy (EDS), confirming the formation of well-aligned nanowire bundles with uniform elemental distribution. The sensor demonstrated a strong and reproducible electrochemical response toward Mg^{2+} ions, exhibiting a high sensitivity of 3.44 µA/µM within a linear detection range of 0–120 µM. The limit of detection (LOD) was calculated to be 7.25 µM, indicating the sensor's capability to detect trace levels of magnesium with precision. These electrochemical properties are attributed to the high surface area of the $ZnCO_x$ nanostructures, efficient electron transfer at the electrode–electrolyte interface, and favorable adsorption behavior of Mg^{2+} ions on the modified surface. The $ZnCO_x$/Ni-foam sensor also benefits from a straightforward fabrication process, mechanical robustness, and chemical stability, making it an attractive platform for the development of practical sensing devices. Given its high sensitivity, low detection limit, and reliable performance, the sensor shows significant promise for real-world applications, particularly in monitoring magnesium content in complex matrices such as agricultural soil or environmental water samples. Future studies will focus on the sensor's selectivity in the presence of competing ions, long-term stability, and integration into portable electrochemical detection systems.

DECLARATIONS

Ethical Approval

We affirm that this manuscript is an original work, has not been previously published, and is not currently under consideration for publication in any other journal or conference proceedings. All authors have reviewed and approved the manuscript, and the order of authorship has been mutually agreed upon.

Funding

Not applicable

Availability of data and material

All of the data obtained or analyzed during this study is

© Ariston Publications 2025. All rights reserved.

included in the report that was submitted.

Conflicts of Interest

The authors declare that they have no financial or personal interests that could have influenced the research and findings presented in this paper. The authors alone are responsible for the content and writing of this article.

Author's contribution statement

All authors contributed equally to this work.

ACKNOWLEDGEMENTS

The authors express their gratitude to the SERB DST, New Delhi, India for providing financial assistance under the Young Scientist scheme (SR/FTP/PS-041/2012). Additionally, the authors are grateful for the financial support received from the Rajiv Gandhi Science & Technology Commission (RGSTC), Government of Maharashtra and Vice Chancellor Research Motivational Scheme (VCRMS) through Kavayitri Bahinabai Chaudhari North Maharashtra University, Jalgaon (KBCNMU/RGSTC/Sanction Order/ 34 (Project code No.: 35-LSR) and (KBCNMU/11A/ VCRMS/ Budget-2022-23/133/2023).

REFERENCES

[1] Marschner, H., **2012**. *Marschner's mineral nutrition of higher plants*. Academic press.

[2] Brady, N. C., Weil, R. R., & Weil, R. R., **2008**. *The nature and properties of soils*, Vol. 13, pp. 662-710. Upper Saddle River, NJ: Prentice Hall.

[3] Epstein, E., & Bloom, A. J., **2005**. *Mineral nutrition of plants: principles and perspectives*. Sinauer.

[4] Lindsay, W., **1979**. *Chemical equilibria in soils*. John Wiley and Sons.

[5] Ahmad, M., Waraich, E. A., Shahid, H., Ahmad, Z., Zulfiqar, U., Mahmood, N., & El Sabagh, A., **2023**. Exogenously Applied Potassium Enhanced Morpho-Physiological Growth and Drought Tolerance of Wheat by Alleviating Osmotic Imbalance and Oxidative Damage. *Polish Journal of Environmental Studies*, 32(5), pp. 4447-4459.

[6] Ramane, D. V., Patil, S. S., & Shaligram, A. D., **2015**, February. Detection of NPK nutrients of soil using Fiber Optic Sensor. In *International Journal of Research in Advent Technology Special Issue National Conference ACGT 2015*, pp. 13-14.

[7] Burton, L., Dave, N., Fernandez, R. E., Jayachandran, K., & Bhansali, S., **2018**. Smart gardening IoT soil sheets for real-time nutrient analysis. *Journal of The Electrochemical Society*, 165(8), B3157.

[8] Behera, S. K., & Shukla, A. K., **2015**. Spatial distribution of surface soil acidity, electrical conductivity, soil organic carbon content and exchangeable potassium, calcium and magnesium in some cropped acid soils of India. *Land Degradation & Development*, 26(1), 71-79.

[9] Lemos, S. G., Nogueira, A. R. A., Torre-Neto, A., Parra, A., & Alonso, J., **2007**. Soil calcium and pH monitoring sensor system. *Journal of Agricultural and Food Chemistry*, 55(12), 4658-4663.

[10] Nag, A., Mukhopadhyay, S. C., & Kosel, J., **2017**. Sensing system for salinity testing using laser-induced graphene sensors. *Sensors and Actuators A: Physical*, 264, 107-116.

[11] Alahi, M. E. E., Nag, A., Mukhopadhyay, S. C., & Burkitt, L., **2018**. A temperature-compensated graphene sensor for nitrate monitoring in real-time application. *Sensors and Actuators A: Physical*, 269, 79-90.

[12] Kim, H. J., Sudduth, K. A., & Hummel, J. W., **2009**. Soil macronutrient sensing for precision agriculture. *Journal of Environmental Monitoring*, 11(10), 1810-1824.

[13] Sparks, D. L., **2003**. Environmental soil chemistry: An overview. *Environmental soil chemistry*, 2, 1-42.

[14] Rayment, G. E., & Lyons, D. J., **2011**. *Soil chemical methods: Australasia*, Vol. 3. CSIRO publishing.

[15] Jones, J. B., **2001**. *Laboratory guide for conducting soil tests and plant analysis*. CRC press.

[16] Khan, S. R., Sharma, B., Chawla, P. A., & Bhatia, R., **2022**. Inductively coupled plasma optical emission spectrometry (ICP-OES): a powerful analytical technique for elemental analysis. *Food Analytical Methods*, 1-23.

[17] Marguí, E., Queralt, I., & De Almeida, E., **2022**. X-ray fluorescence spectrometry for environmental analysis: Basic principles, instrumentation, applications and recent trends. *Chemosphere*, 303, 135006.

[18] Kilbride, C., Poole, J., & Hutchings, T. R., **2006**. A comparison of Cu, Pb, As, Cd, Zn, Fe, Ni and Mn determined by acid extraction/ICP–OES and ex situ field portable X-ray fluorescence analyses. *Environmental Pollution*, 143(1), 16-23.

[19] Rhoades, J. D., **1982**. Soluble salts. *Methods of soil analysis: Part 2 chemical and microbiological properties*, 9, 167-179.

© Ariston Publications 2025. All rights reserved.

[20] Nag, A., Mukhopadhyay, S. C., & Kosel, J., **2017**. Sensing system for salinity testing using laser-induced graphene sensors. *Sensors and Actuators A: Physical*, 264, 107-116.

[21] Alahi, M. E. E., Nag, A., Mukhopadhyay, S. C., & Burkitt, L., **2018**. A temperature-compensated graphene sensor for nitrate monitoring in real-time application. *Sensors and Actuators A: Physical*, 269, 79-90.

[22] Afsarimanesh, N., Alahi, M. E. E., Mukhopadhyay, S. C., & Kruger, M., **2018**. Development of IoT-based impedometric biosensor for point-of-care monitoring of bone loss. *IEEE Journal on Emerging and Selected Topics in Circuits and Systems*, 8(2), 211-220.

[23] Piccinno, F., Gottschalk, F., Seeger, S., & Nowack, B., **2012**. Industrial production quantities and uses of ten engineered nanomaterials in Europe and the world. *Journal of nanoparticle research*, 14, 1-11.

[24] Cai, W., **2024**. Functional Nanomaterials for Sensing and Detection. *Nanomaterials*, 14(1), 128.

[25] Khan, S. T., Adil, S. F., Shaik, M. R., Alkhathlan, H. Z., Khan, M., & Khan, M., **2021**. Engineered nanomaterials in soil: their impact on soil microbiome and plant health. *Plants*, 11(1), 109.

[26] Che, H., Liu, A., Zhang, X., Mu, J., Bai, Y., & Hou, J., **2015**. Three-dimensional hierarchical ZnCo2O4 flower-like microspheres assembled from porous nanosheets: Hydrothermal synthesis and electrochemical properties. *Ceramics International*, 41(6), 7556-7564.

[27] Singh, D. P., **2010**. Synthesis and growth of ZnO nanowires. *Science of advanced materials*, 2(3), 245-272.

[28] Liu, T., Liu, J., Liu, Q., Song, D., Zhang, H., Zhang, H., & Wang, J., **2015**. Synthesis, characterization and enhanced gas sensing performance of porous ZnCo 2 O 4 nano/microspheres. *Nanoscale*, 7(46), 19714-19721.

[29] Kumar, R., **2020**. $NiCo_2O_4$ nano-/microstructures as high-performance biosensors: a review. *Nano-micro letters*, 12, 1-52.

[30] El-Hout, S. I., Chen, C., Liang, T., Yang, L., & Zhang, J., **2017**. Cetyltrimethylammonium bromide assisted hydrothermal synthesis of cobalt oxide nanowires anchored on graphene as an efficient electrode material for supercapacitor applications. *Materials Chemistry and Physics*, 198, 99-106.

[31] Mammadyarova, S. J., **2021**. Synthesis and characterization of cobalt oxide nanostructures a brief review. *Azerbaijan Chemical Journal*, (2), 80-93.

[32] Zhang, M., & Gorski, W., **2005**. Electrochemical sensing based on redox mediation at carbon nanotubes. *Analytical chemistry*, 77(13), 3960-3965.

[33] Montgomery, D. C., **2017**. *Design and analysis of experiments*. John wiley & sons.

[34] Zhong, C., Deng, Y., Hu, W., Qiao, J., Zhang, L., & Zhang, J., **2015**. A review of electrolyte materials and compositions for electrochemical supercapacitors. *Chemical Society Reviews*, 44(21), 7484-7539.

[35] Gurira, R. C., & Bowers, L. D., **1983**. Electrochemistry of methotrexate: Part I. Characteristics of reduction. *Journal of Electroanalytical Chemistry and Interfacial Electrochemistry*, 146(1), 109-122.

[36] Ding, Q., Li, C., Wang, H., Xu, C., & Kuang, H., **2021**. Electrochemical detection of heavy metal ions in water. *Chemical Communications*, 57(59), 7215-7231.

[37] Qiu, J., Li, X., He, W., Park, S. J., Kim, H. K., Hwang, Y. H., ... & Kim, Y. D., **2009**. The growth mechanism and optical properties of ultralong ZnO nanorod arrays with a highaspect ratio by a preheating hydrothermal method. *Nanotechnology*, 20(15), 155603.

[38] Janotti, A., & Van de Walle, C. G., **2009**. Fundamentals of zinc oxide as a semiconductor. *Reports on progress in physics*, 72(12), 126501.

[39] Mohamad Nor, N., Ramli, N. H., Poobalan, H., Qi Tan, K., & Abdul Razak, K., **2023**. Recent advancement in disposable electrode modified with nanomaterials for electrochemical heavy metal sensors. *Critical reviews in analytical chemistry*, 53(2), 253-288.

[40] Lei, C., Pi, M., Jiang, C., Cheng, B., & Yu, J., **2017**. Synthesis of hierarchical porous zinc oxide (ZnO) microspheres with highly efficient adsorption of Congo red. *Journal of colloid and interface science*, 490, 242-251.

 © Ariston Publications 2025. All rights reserved.